

## Suppression of hybridization by Cd doping in CeCoIn<sub>5</sub>

Q. Y. Chen<sup>1,\*</sup>, F. Ronning<sup>2</sup>, E. D. Bauer<sup>2</sup>, C. H. P. Wen<sup>3</sup>, Y. B. Huang<sup>4</sup>, and D. L. Feng<sup>3,5,6</sup>

<sup>1</sup>Science and Technology on Surface Physics and Chemistry Laboratory, Mianyang 621908, China

<sup>2</sup>Los Alamos National Laboratory, Los Alamos, New Mexico 87545, USA

<sup>3</sup>State Key Laboratory of Surface Physics and Department of Physics, Fudan University, Shanghai 200433, China

<sup>4</sup>Shanghai Institute of Applied Physics, CAS, Shanghai, 201204 China

<sup>5</sup>Hefei National Laboratory for Physical Science at Microscale, CAS Center for Excellence in Quantum Information and Quantum Physics, and Department of Physics, University of Science and Technology of China, Hefei 230026, People's Republic of China

<sup>6</sup>Collaborative Innovation Center of Advanced Microstructures, Nanjing 210093, People's Republic of China



(Received 9 June 2019; revised manuscript received 15 October 2019; published 30 December 2019)

The interaction between superconductivity and magnetism in heavy fermion compounds has remained a challenge ever since the discovery of unconventional superconductivity in such systems. The heavy fermion CeTIn<sub>5</sub> ( $T = \text{Co, Rh, Ir}$ ) family offers a good platform to study the relationship between superconductivity and magnetism, whose ground state can be easily tuned by chemical doping, making the ambient-pressure experimental techniques like angle-resolved photoemission spectroscopy possible to address this old but engaging question. By Cd doping, the superconducting state of CeCoIn<sub>5</sub> can be smoothly tuned to an antiferromagnetic ground state, which can be reversed by applying pressure. Here we present an electronic structure study of CeCo(In<sub>0.85</sub>Cd<sub>0.15</sub>)<sub>5</sub> with an antiferromagnetic ground state and the results are compared with CeCoIn<sub>5</sub>. We found that the hybridization strength between the  $f$  electrons and conduction electrons in CeCoIn<sub>5</sub> has been suppressed by Cd doping, but still the Fermi surface includes a significant contribution from the Ce  $f$  electrons. Our results find that the electronic tuning effect by Cd doping arises from the change in the hybridization strength between the Ce  $f$  electrons and conduction electrons caused by the Cd dopant, and the subtle interplay between itinerancy and localization of the  $f$  electrons determines the ground state.

DOI: [10.1103/PhysRevB.100.235148](https://doi.org/10.1103/PhysRevB.100.235148)

### I. INTRODUCTION

Understanding the interactions between superconductivity and magnetism in heavy fermion compounds has remained a challenge ever since the discovery of unconventional superconductivity. The comparatively high tunability of the heavy fermions in cerium- and ytterbium-based rare earth intermetallics makes them attractive systems in the search for emergent phases of matter [1]. Due to the dynamic generation of comparatively small energy scales, the ground state of the heavy-fermion system can be easily tuned by pressure, magnetic field, or chemical doping [2]. The family of the heavy fermion compounds CeTIn<sub>5</sub> ( $T = \text{Co, Rh, Ir}$ ) has proven fertile for the study of heavy-fermion ground states and the interplay between antiferromagnetism and superconductivity [3–7]. Among them, CeCoIn<sub>5</sub> is a star member with the relatively high superconducting transition temperature of 2.3 K, and has been intensively studied by various experimental techniques and theoretical calculations [8–14].

By Cd doping in CeCoIn<sub>5</sub>, the ground state can be smoothly tuned from a superconducting state to an antiferromagnetic state, which can be driven back by applying pressure. The superconducting transition temperature remains nearly constant with increasing Cd substitu-

tion up to  $x = 0.5\%$  in pure CeCoIn<sub>5</sub>. Superconductivity coexists with the antiferromagnetic order for  $x = 0.5\% < x \leq 1.25\%$ , after which point only antiferromagnetic order is observed [15,16]. The magnetic order found in Cd-doped CeCoIn<sub>5</sub> is commensurate [17], which contrasts with the incommensurate magnetic structure found in the related antiferromagnet CeRhIn<sub>5</sub> [18]. It is still an open question how Cd induces the long-range antiferromagnetic order with a large ordered magnetic moment.

The specific heat of CeCo(In<sub>1-x</sub>Cd<sub>x</sub>)<sub>5</sub> has been studied by Tokiwa *et al.* [15]. Local structure and site occupancy of Cd substitution in CeCoIn<sub>5</sub> has been examined by the extended x-ray absorption fine-structure (EXAFS) technique [19]. de Haas–van Alphen (dHvA) measurements revealed a small but systematic change in the dHvA frequencies with Cd doping, reflecting the chemical potential shift due to the removal of conduction electrons, and they also observed no abrupt change of the Fermi surface (e.g., from “large” to “small”) through the change in the ground state [20]. Gofryk *et al.* [21] found that the nominally nonmagnetic dopants only have a remarkably weak pair breaking effect for a  $d$ -wave superconductor. They also suggest that Cd does not induce any valence fluctuation on neighboring Ce atoms, as originally assumed in order to explain the reversible tuning [22]. A combined study by muon spin rotation, neutron scattering, and x-ray absorption spectroscopy techniques indicates the itinerant character of the magnetic order, which coexists with the bulk superconductivity [23].

\*sheqiyun@126.com

Many previous results suspected that the richness and complexity of the properties observed in the Ce115 compounds come from the Fermi-surface details, in which Kondo and coherence scales are central [8,10–14,24]. Angle-resolved photoemission spectroscopy (ARPES) offers a direct way to observe the electronic structure at various temperatures and can determine both the shape and size of the Fermi surface. Doping Cd in CeCoIn<sub>5</sub> sensitively shifts the balance between superconductivity and antiferromagnetism and opens new ambient-pressure phase space in the study of heavy-fermion ground states [16], making it possible for ARPES to systematically study the evolution of the electronic structure from superconducting state to antiferromagnetic state, which is still lacking now. In our previous study of CeCoIn<sub>5</sub>, we have directly observed the localized-to-itinerant transition of the *f* electrons as the temperature is lowered [25]. Revealing the difference of the electronic structure between CeCoIn<sub>5</sub> and the Cd-doped samples turns out to be important for understanding fully the relationship between superconductivity and antiferromagnetism. Here we present an electronic structure study of the Cd-doped samples, which aims at elucidating the origin of the changes for different ground states from an electronic-structure point of view.

In the present study, we provide an electronic structure study of CeCo(In<sub>1-x</sub>Cd<sub>x</sub>)<sub>5</sub> with the nominal doping concentration of 0.15, whose ground state is antiferromagnetic. The actual Cd concentration is approximately 10 times smaller. Three dimensional Fermi surface and band structure are revealed and suggest rather three-dimensional character of this compound. The conduction bands of CeCo(In<sub>0.85</sub>Cd<sub>0.15</sub>)<sub>5</sub> are almost identical to that of CeCoIn<sub>5</sub>, albeit an obvious difference can be found for the low-energy excitations. The extent of the hybridization between the *f* electrons and conduction electrons has been decreased by Cd doping; still the Fermi surface includes a significant contribution from the *f* electrons. Our results provide direct evidence that the subtle interplay of itinerancy and localization of *f* electrons determines the ground state of CeCoIn<sub>5</sub>.

## II. EXPERIMENTAL DETAILS

All single crystals were grown by the indium self-flux method. The doping levels were determined by single crystal x-ray diffraction and microprobe analysis [21]. Room-temperature x-ray diffraction measurements reveal that all the crystals are single phase and crystallize in the tetragonal HoCoGa<sub>5</sub> structure. The samples were cleaved along the *c* axis before performing ARPES measurements. ARPES measurements were performed at the “Dreamline” beamline of the Shanghai Synchrotron Radiation Facility (SSRF) with a Scienta DA30 analyzer. Both LV- and LH-polarized photons were used. The vacuum was better than  $5 \times 10^{-11}$  mbar at 18 K. The energy resolution was 17 meV for 121 eV photons, and the angular resolution was 0.2°.

## III. RESULTS AND DISCUSSIONS

Figure 1(a) presents the three dimensional Brillouin zone of CeCo(In<sub>0.85</sub>Cd<sub>0.15</sub>)<sub>5</sub> with all the high symmetry planes and points indicated. Experimental setup for our ARPES

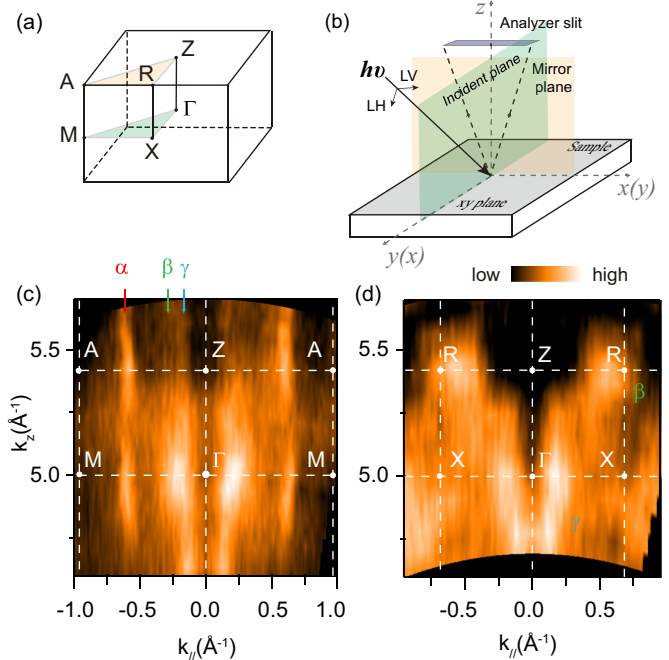


FIG. 1. (a) Brillouin zone of CeCo(In<sub>0.85</sub>Cd<sub>0.15</sub>)<sub>5</sub>. (b) Experimental setup for ARPES measurements. (c) Photoemission intensity map in the  $\Gamma ZAM$  plane. (d) Photoemission intensity map in the  $\Gamma ZRX$  plane. All photoemission intensity data here were integrated over a window of  $(E_F - 20 \text{ meV}, E_F + 20 \text{ meV})$ .

measurements is shown in Fig. 1(b). Photoemission intensity maps in the  $\Gamma ZAM$  and  $\Gamma ZRX$  planes of the Cd-doped samples are shown in Figs. 1(c) and 1(d), respectively. From Fig. 1(c), three bands can be resolved contributing to the Fermi surface of CeCo(In<sub>0.85</sub>Cd<sub>0.15</sub>)<sub>5</sub>, named  $\alpha$ ,  $\beta$ , and  $\gamma$ . It is similar to that observed in the parent compound CeCoIn<sub>5</sub> [25]. Among the three bands, the dispersion of the  $\alpha$  band can be clearly traced, which is nearly cylindrical along the  $k_z$  direction with rather two-dimensional character. For the  $\gamma$  Fermi surface, its dispersion is hard to trace in the  $\Gamma ZAM$  plane, showing rather strong  $k_z$  dependence. In the  $\Gamma ZRX$  plane, a hole pocket can be found around the  $\Gamma$  point, which is from the  $\gamma$  Fermi surface. Also, some spectral weight can be observed around the *R* point, which comes from the  $\beta$  Fermi surface. From the dispersion of the  $\beta$  band, part of the Fermi surface shows two dimensional character, which is evident by the corrugated cylindrical sheets observed around the *M* point along the  $k_z$  direction, while part of the Fermi surface is three dimensional, which has contribution in the *ZAR* plane and is absent in the  $\Gamma XM$  plane. These results suggest that both the  $\beta$  and  $\gamma$  bands are rather three dimensional. This is consistent with dHvA measurements and theoretical calculations. They also observed three Fermi surfaces, and the  $\alpha$  Fermi surface is the most two dimensional one [26].

Figure 2(a) displays the photoemission intensity map of CeCo(In<sub>0.85</sub>Cd<sub>0.15</sub>)<sub>5</sub> at 18 K taken with 85 eV photons. The Fermi surface consists of two Fermi pockets around the Brillouin zone corner—a flower-shaped  $\beta$  pocket and a squarelike  $\alpha$  pocket. Also a small squarelike Fermi pocket can be observed around the zone center, which is part of

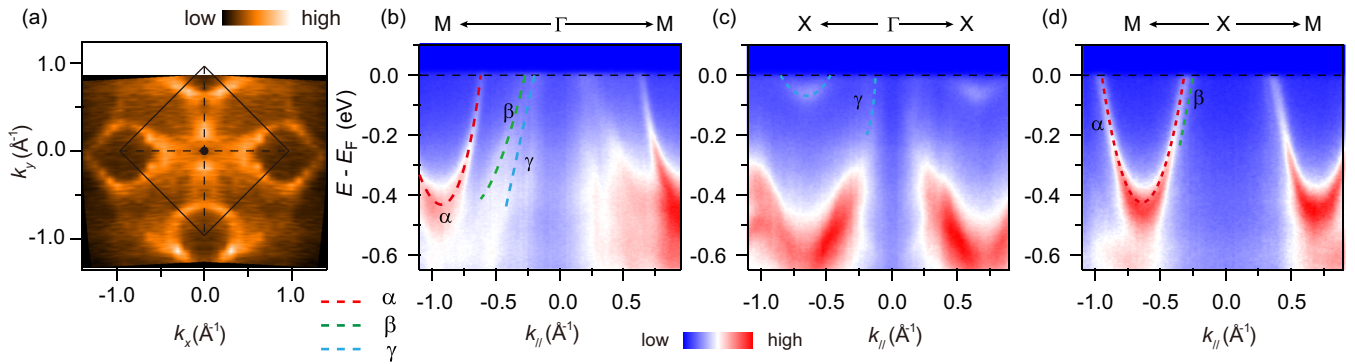


FIG. 2. Fermi surface and band structure of  $\text{CeCo}(\text{In}_{0.85}\text{Cd}_{0.15})_5$  taken with 85 eV LV-polarized photons at 18 K. (a) Photoemission intensity map of  $\text{CeCo}(\text{In}_{0.85}\text{Cd}_{0.15})_5$  integrated over a window of  $(E_F - 20 \text{ meV}, E_F + 20 \text{ meV})$ . (b)–(d) Photoemission intensity distributions along (b)  $\Gamma$ - $M$ , (c)  $\Gamma$ - $X$ , and (d)  $M$ - $X$ .

the  $\gamma$  Fermi surface. One narrow racetrack pocket can be observed extending to the middle of the zone boundary, which is also assigned to the  $\gamma$  band. Detailed band dispersions along several high-symmetry directions can be seen in Figs. 2(b)–2(d). Along the  $\Gamma M$  direction, three bands can be observed crossing the Fermi level, which can be assigned to the  $\alpha$ ,  $\beta$ , and  $\gamma$  bands, respectively. The  $\alpha$  band is parabolic-like with its bottom 0.45 eV below the Fermi level. It is almost identical with that observed in its parent compound  $\text{CeCoIn}_5$  [25], and compared with that of 0.95 eV in  $\text{CeIrIn}_5$  [27]. The holelike  $\gamma$  band encloses the  $\Gamma$  point, which forms the squarelike  $\gamma$  Fermi pocket around the Brillouin zone center.

We next focus on using photons of 121 eV, corresponding to the  $4d$ - $4f$  x-ray absorption edge, which can strongly enhance the contribution and features related to the Ce  $4f$  states [28]. Figures 3(a) and 3(b) show the photoemission intensity plots for  $\text{CeCo}(\text{In}_{0.85}\text{Cd}_{0.15})_5$  taken with 121 eV photons under LV and LH conditions, respectively. From Fig. 3(a), a nearly flat band can be observed located at 2.4 eV binding energy, which shows weak dispersion corresponding to the  $4f^0$  final-state associated with the cost of removing one electron from the trivalent Ce ion ( $4f^1 \rightarrow 4f^0$ ). There are

two other features located at 0.27 eV and 0.02 eV binding energy, and the former is consistent with the spin-orbit split of the  $4f$  states in Ce systems. The latter can be attributed to the  $4f_{5/2}^1$  state, which is the tail of the Kondo resonance and should be above the Fermi level but can be observed in photoemission measurements due to the “final-state” excitations [29], as will be discussed later. Figure 3(b) shows the ARPES data taken with 121 eV LH-polarized photons. From Fig. 3(b), the  $4f^0$  state can also be clearly observed with LH polarization showing no obvious change, while the  $4f_{5/2}^1$  state is quite sensitive to the polarization of the light, which is nearly absent under LH-polarized light. Figure 3(c) shows the ARPES data of  $\text{CeCoIn}_5$  taken under the same conditions as Fig. 3(a). An obvious difference can be found between the Cd-doped samples and the parent compound  $\text{CeCoIn}_5$ . The intensity of the  $4f^0$  state is rather weak in  $\text{CeCoIn}_5$  with only a small hump at 2.2 eV, and also the spectral weight of the  $f$  states near the Fermi level turns out to be very strong in  $\text{CeCoIn}_5$ .

To show the detailed difference between  $\text{CeCo}(\text{In}_{0.85}\text{Cd}_{0.15})_5$  and  $\text{CeCoIn}_5$ , Figs. 4(a) and 4(b) zoom into the vicinity near the Fermi level. From Figs. 4(a) and 4(b), the conduction bands away from the Fermi level

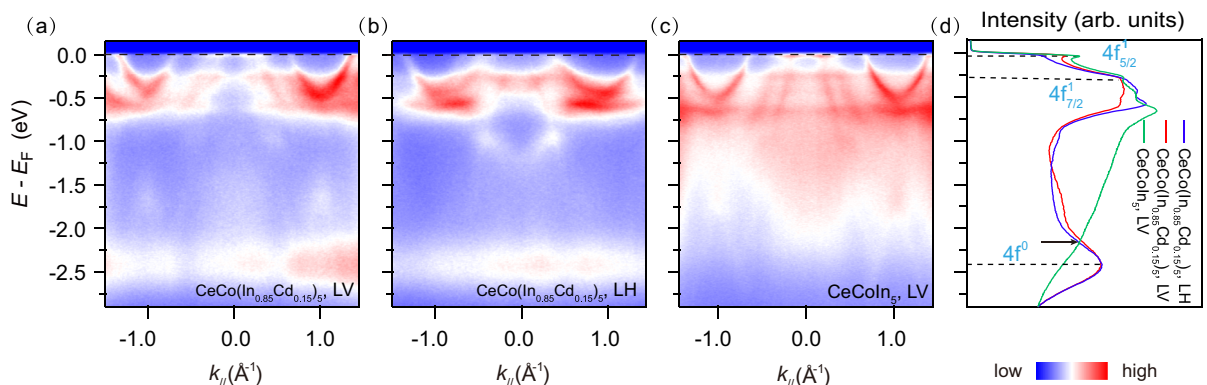


FIG. 3. Photoemission intensity distributions of  $\text{CeCo}(\text{In}_{0.85}\text{Cd}_{0.15})_5$  along  $\Gamma$ - $M$  taken at 18 K with (a) 121 eV LV-polarized photons and (b) LH-polarized photons. (c) Photoemission intensity distributions of  $\text{CeCoIn}_5$  along  $\Gamma$ - $M$  taken at 17 K with LV-polarized photons, as can be found in Ref. [25]. (d) Angle-integrated EDCs of  $\text{CeCo}(\text{In}_{0.85}\text{Cd}_{0.15})_5$  and  $\text{CeCoIn}_5$ ; the  $f$ -band positions are highlighted. The small hump in  $\text{CeCoIn}_5$  which is supposed to be the  $4f^0$  state is marked with a black arrow. The spectra have been normalized by the intensity at 2.8 eV binding energy.

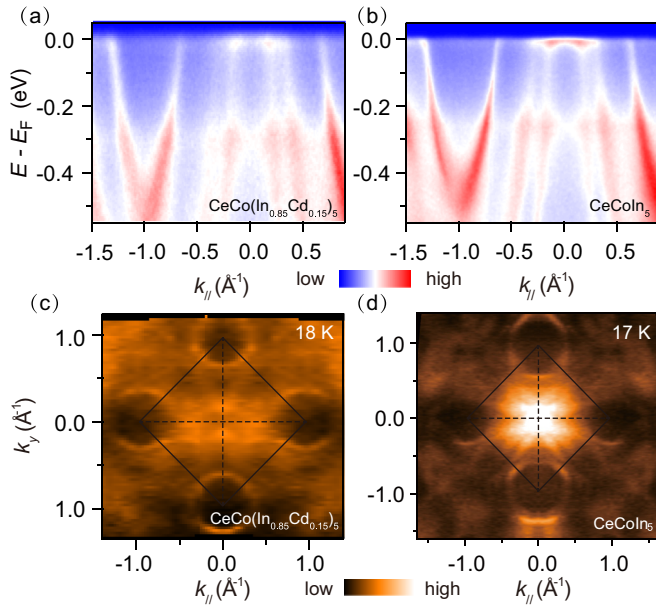


FIG. 4. (a) Photoemission intensity distributions of  $\text{CeCo}(\text{In}_{0.85}\text{Cd}_{0.15})_5$  along  $\Gamma$ - $M$  taken at 18 K. (b) Photoemission intensity distributions of  $\text{CeCoIn}_5$  along  $\Gamma$ - $M$  taken at 17 K, as can also be found in Ref. [25]. (c) Photoemission intensity map of  $\text{CeCo}(\text{In}_{0.85}\text{Cd}_{0.15})_5$  along  $\Gamma$ - $M$  taken at 18 K. (d) Photoemission intensity map of  $\text{CeCoIn}_5$  along  $\Gamma$ - $M$  taken at 17 K, as can also be found in Ref. [25].

are almost identical in the two compounds, while difference can be found between the two compounds for the low-energy electronic structure and the  $f$  bands. In  $\text{CeCoIn}_5$ , a weakly dispersive band can be clearly observed near the Fermi level around the  $\Gamma$  point, resulting from the hybridization

between the  $f$  electrons and conduction electrons, while, by Cd doping, the intensity of this feature has been obviously suppressed, indicating the decreased extent of the average hybridization between the  $f$  band and the conduction bands. But still the  $f$  spectral weight can be found in the Cd-doped samples, which can be more clearly observed from Fig. 4(a) and suggests that the  $f$  electrons also participate in the Fermi surface construction in  $\text{CeCo}(\text{In}_{0.85}\text{Cd}_{0.15})_5$ . We did not observe obvious difference for the  $\alpha$  band in the two compounds. Figures 4(c) and 4(d) display the photoemission intensity maps of  $\text{CeCo}(\text{In}_{0.85}\text{Cd}_{0.15})_5$  and  $\text{CeCoIn}_5$ , from which it is clear that the  $f$  spectral weight mainly locates near the Brillouin zone center in  $\text{CeCoIn}_5$ , and an obvious suppression can be observed by Cd doping for this feature. It is noteworthy that the energy resolution for our ARPES measurements is around 17 meV. It is reasonable to expect that the difference should be more obvious with better energy resolution, which can better illustrate the key physics close to the Fermi level.

To investigate the evolution of the  $f$  states as a function of temperature, we performed temperature-dependent resonant ARPES measurements with 121 eV LV-polarized photons along the  $\Gamma M$  direction. Figure 5 displays the temperature evolution of the three bands. From Fig. 5(a), a weakly dispersive feature can be found near the Fermi level around the  $\Gamma$  point. Upon increasing temperature, the intensity of this spectral weight gradually decreases and nearly disappears at 110 K, which can be further illustrated by the EDCs around the  $\Gamma$  point in Fig. 5(b). Figure 5(c) shows the evolution of the  $\alpha$  band with temperature. At 110 K, the  $\alpha$  band shows linear dispersion, while at low temperature, a slight bending is observed for this band near the Fermi energy, which is an indication of the hybridization between this band and the  $f$  band. It is noteworthy that the  $c$ - $f$  hybridization displays a

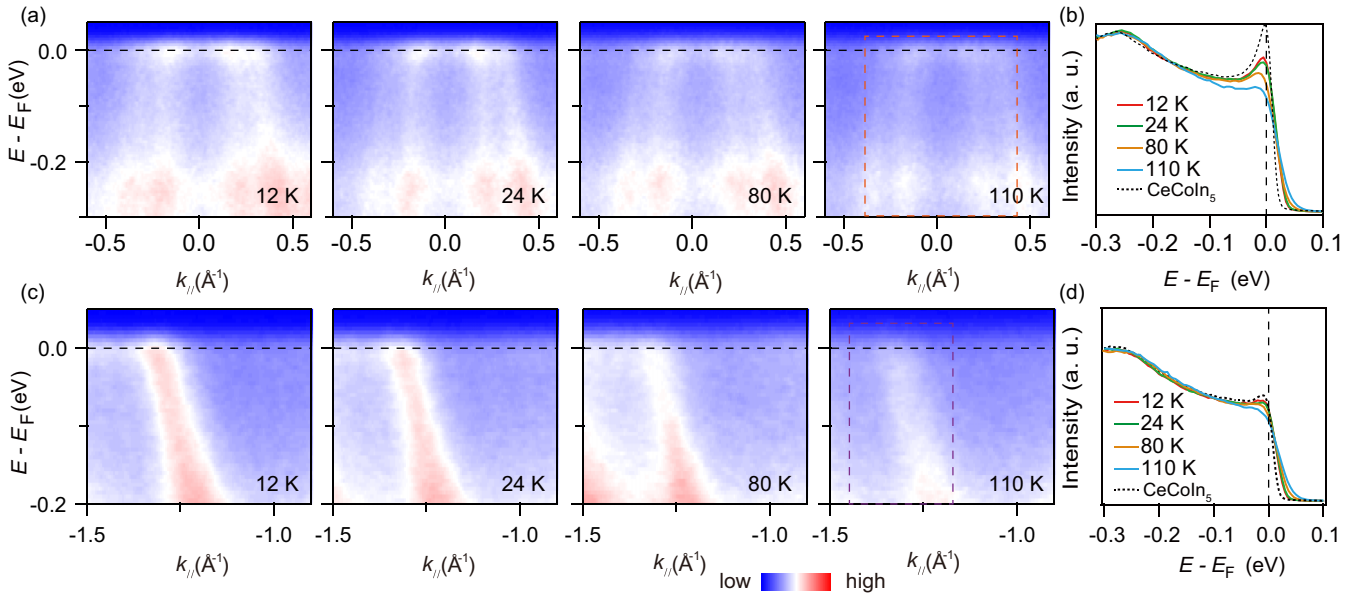


FIG. 5. Temperature evolution of the electronic structure of  $\text{CeCo}(\text{In}_{0.85}\text{Cd}_{0.15})_5$ . (a) Zoomed-in ARPES data of the  $\beta$  and  $\gamma$  bands along  $\Gamma$ - $M$  at the temperatures indicated. (b) Temperature dependence of the EDCs around the  $\Gamma$  point. The integrated window is marked with the red dashed block. (c) The same as (a), but for the  $\alpha$  band. (d) Temperature dependence of the EDCs around the left part of the  $\alpha$  band. The integrated window is marked with the purple dashed block. The dashed lines in (b) and (c) denote the EDCs of  $\text{CeCoIn}_5$  taken at 17 K.

clear band dependence. The EDCs for the  $\gamma$  band show more obvious change in Fig. 5(b), comparing with that for the  $\alpha$  band in Fig. 5(d), suggesting that the most two dimensional  $\alpha$  band shows the weakest hybridization, while the most three dimensional  $\gamma$  band shows the strongest hybridization in  $\text{CeCo}(\text{In}_{0.85}\text{Cd}_{0.15})_5$ . In  $\text{CeCoIn}_5$ , there are two In sites: In(1) and In(2). The former is in the same plane as the Ce atoms and the latter is out of plane. Previous EXAFS study on Cd substitution in  $\text{CeTIn}_5$  ( $T = \text{Co, Rh, Ir}$ ) by Booth *et al.* observed the strong preference for Cd substitution to occupy the In(1) site than the out-of-plane In(2) site [19]. Since the local environment around the In(1) site has a shorter nearest-neighbor distance than the In(2) site, it is not surprising that a given substituent onto the In sites would prefer the In(1) site. This site-dependent effect may also cause the corresponding band-dependent hybridization effect, which still needs further theoretical considerations in the future.

In the family of Ce115 compounds, the cleaving process may result in the exposure of multiple surface terminations with different chemical compositions. Previous STM results on many cleaved samples of  $\text{CeCoIn}_5$  revealed three different surfaces, two of which are atomically ordered, and the third surface is reconstructed [9]. This makes it difficult to get a monotermination within the beam spot size for our ARPES measurements, so the effect of sample surface quality may also be a possible reason for the observed reduction in  $f$ -spectral weight for the Cd-doped samples. It is difficult to evaluate the effect of sample surface quality very accurately. However, from Figs. 5(b) and 5(d), we found that suppression of the  $f$  spectral weight by Cd doping is much greater for the  $\gamma$  band than for the  $\alpha$  band, which offers us a plausible way to correct the extrinsic effects due to different sample surface quality. If we assume that suppression of the  $f$ -spectral weight for the  $\alpha$  band by Cd doping is entirely due to the extrinsic surface quality effects, this can be used as a background for the  $\gamma$  band to correct the extrinsic effect. In Fig. S1 of the Supplemental Material [30], we have plotted the  $f$  spectral weight for the  $\gamma$  band in both  $\text{CeCoIn}_5$  and  $\text{CeCo}(\text{In}_{0.85}\text{Cd}_{0.15})_5$  after subtracting the background of the  $\alpha$  band. After this attempt to correct for the extrinsic effects, there is still an intrinsic reduction of  $f$ -spectral weight suppression for the  $\gamma$  band by Cd doping in Fig. S1(f), which further demonstrates the suppression of hybridization by Cd doping in  $\text{CeCoIn}_5$ . The suppression of  $f$ -spectral weight for different bands by Cd doping also indicates the existence of orbital-selective  $f$ -spectral weight in this compound.

In this work, we observed suppression of the hybridization between the  $f$  electrons and conduction electrons by Cd doping in  $\text{CeCoIn}_5$ . Still, some  $f$  spectral weight can be found near the Fermi level, indicating the existence of an itinerant component of the  $f$  electrons in  $\text{CeCo}(\text{In}_{0.85}\text{Cd}_{0.15})_5$ . In our previous study of  $\text{CeCoIn}_5$ , we found that the Fermi volume increase is much smaller than DMFT predictions [32] and the  $f$  electrons become only partially itinerant [25]. From the comparison of the ARPES data between  $\text{CeCo}(\text{In}_{0.85}\text{Cd}_{0.15})_5$  and  $\text{CeCoIn}_5$ , fewer  $f$  electrons take part in the formation of the Fermi surface by Cd doping. These results suggest that only a fraction of the  $f$  electrons in  $\text{CeCo}(\text{In}_{0.85}\text{Cd}_{0.15})_5$  participates in the construction of the Fermi surface, and the  $f$  electrons show dual character. The local spin of the  $f$

electrons is only partially screened by the surrounding conduction electrons, which enables the appearance of the long-range order driven by the unscreened part of the spin. The magnetism is driven by the RKKY interactions between not yet fully hybridized local  $f$  spins, while part of the Ce  $4f$  electrons remains well hybridized with the conduction electrons as can be evident from the obvious  $f$  spectral weight near the Fermi level in  $\text{CeCo}(\text{In}_{0.85}\text{Cd}_{0.15})_5$ . These results agree with the dHvA measurements, which also support no abrupt change of the Fermi surface from large to small accompanies the change in the ground state from the superconducting state to the antiferromagnetic state [22]. Also density functional theory (DFT) found that the Cd  $p$  states possess a smaller bandwidth and are shifted up in energy relative to the In states they replaced, supporting the decreased hybridization observed by Cd doping [21]. This can also explain why the effect of Cd doping can be reversed by applying pressure, considering that the application of pressure tends to increase the hybridization between the  $f$  electrons and conduction electrons.

Previous dHvA measurements found no evidence for the enhancement of the effective mass in Cd-doped samples, and they suggest that the added holes by Cd doping in  $\text{CeCoIn}_5$  are mainly distributed over the remaining pieces of the Fermi surface, which they did not observe [22]. This can be evident by our results. From our ARPES measurements, we find weaker  $f$  spectral weight for the  $\alpha$  band and weaker difference between pure  $\text{CeCoIn}_5$  and the Cd-doped samples for the  $\alpha$  band's  $f$  spectral weight. Due to the low frequency of the  $\gamma$  band, changes of the shape and size of the  $\gamma$  pocket cannot be provided by dHvA measurements, and they are primarily for the  $\alpha$  and  $\beta$  sheets only, which show weaker hybridization. This band-dependent behavior is also consistent with the anisotropic hybridization by x-ray absorption spectroscopy [33], and makes it possible for doping dependent renormalization effects to be band dependent.

Our results demonstrate that the changes of the ground states that occur in  $\text{CeCoIn}_5$  with doping or pressure are more likely associated with the Kondo effect and the extent of the hybridization between the  $f$  electrons and conduction electrons. The  $f$  electrons in  $\text{CeCo}(\text{In}_{0.85}\text{Cd}_{0.15})_5$  have a character between local moments and itinerant electrons. This is reasonable, considering the hybridization between the  $f$  bands and conduction bands is band dependent and happens in different parts of the momentum space. The Kondo interaction can coexist with the magnetic order by separating themselves in momentum space with different bands. This coexistence of the magnetic order with the heavy quasiparticles can also be found in Ce-based heavy-fermion compounds  $\text{CeSb}$ ,  $\text{CeRhIn}_5$  [29,34] and U-based compounds  $\text{USb}_2$  [35] as well.

The magnetic order found in Cd-doped  $\text{CeCoIn}_5$  is commensurate [17], which contrasts with the incommensurate magnetic structure found in the related antiferromagnet  $\text{CeRhIn}_5$  [18]. Previous nuclear magnetic resonance results observed satellite peaks in Cd-doped  $\text{CeCoIn}_5$ , which reveals a real space inhomogeneity [36,37]. Cd doping was shown to only locally suppress the hybridization, while most of the sample still recognizes an electronic structure that is representative of a "large" Fermi surface found in pure  $\text{CeCoIn}_5$ . Eventually, the few local magnetic droplets around

the Cd sites drag the near quantum critical system into an antiferromagnetic state. Because the various bands in momentum space have different atomic character, it seems reasonable to expect that this local suppression of hybridization would generate the band dependent hybridization behavior we observed by ARPES and might be the origin of the different behavior between CeRhIn<sub>5</sub> and Cd-doped CeCoIn<sub>5</sub>.

#### IV. CONCLUSION

In summary, we present an electronic structure study of CeCo(In<sub>0.85</sub>Cd<sub>0.15</sub>)<sub>5</sub> with an antiferromagnetic ground state. The conduction bands are almost identical with that of CeCoIn<sub>5</sub>, while obvious difference can be found in the low-energy electronic structure. As can be deduced from the reduction of the *f* spectral weight near the Fermi level, the strength of hybridization in CeCoIn<sub>5</sub> has been greatly suppressed by Cd doping; still the Fermi surface of CeCo(In<sub>0.85</sub>Cd<sub>0.15</sub>)<sub>5</sub> includes a significant contribution from

the Ce *f* electrons, indicating the dual character of the *f* electrons. Our results demonstrate that the changes of the ground state are most likely associated with the Kondo effect and the extent of the hybridization between the *f* electrons and conduction electrons. The Fermi surface in CeCo(In<sub>0.85</sub>Cd<sub>0.15</sub>)<sub>5</sub> is large, in contrast to the small Fermi surface found in CeRhIn<sub>5</sub>, suggesting a separate mechanism for the antiferromagnetism.

#### ACKNOWLEDGMENTS

This work is supported by the National Science Foundation of China (Grants No. 11874330 and No. U1630248), the Science Challenge Project (Grant No. TZ2016004), and the National Key Research and Development Program of China (No. 2017YFA0303104). Work at Los Alamos National Laboratory was performed under the auspices of the U.S. Department of Energy, Office of Basic Energy Sciences, Division of Materials Sciences and Engineering, “Quantum Fluctuations in Narrow Band Systems” project.

- 
- [1] P. Coleman and A. H. Nevidomskyy, Frustration and the Kondo effect in heavy fermion materials, *J. Low Temp. Phys.* **161**, 182 (2010).
- [2] G. R. Stewart, Heavy-fermion systems, *Rev. Mod. Phys.* **56**, 755 (1984).
- [3] Y. Chen, W. B. Jiang, C. Y. Guo, F. Ronning, E. D. Bauer, T. Park, H. Q. Yuan, Z. Fisk, J. D. Thompson, and X. Lu, Reemergent Superconductivity and Avoided Quantum Criticality in Cd-Doped CeIrIn<sub>5</sub> Under Pressure, *Phys. Rev. Lett.* **114**, 146403 (2015).
- [4] H. Hegger, C. Petrovic, E. G. Moshopoulou, M. F. Hundley, J. L. Sarrao, Z. Fisk, and J. D. Thompson, Pressure-Induced Superconductivity in Quasi-2D CeRhIn<sub>5</sub>, *Phys. Rev. Lett.* **84**, 4986 (2000).
- [5] A. Llobet, A. D. Christianson, W. Bao, J. S. Gardner, I. P. Swainson, J. W. Lynn, J.-M. Mignot, K. Prokes, P. G. Pagliuso, N. O. Moreno, J. L. Sarrao, J. D. Thompson, and A. H. Lacerda, Novel Coexistence of Superconductivity with Two Distinct Magnetic Orders, *Phys. Rev. Lett.* **95**, 217002 (2007).
- [6] H. Martinho, P. G. Pagliuso, V. Fritsch, N. O. Moreno, J. L. Sarrao, and C. Rettori, Vibrational and electronic excitations in the (Ce, La)MIn<sub>5</sub> (*M* = Co, Rh) heavy-fermion family, *Phys. Rev. B* **75**, 045108 (2007).
- [7] Q. Y. Chen, D. F. Xu, X. H. Niu, R. Peng, H. C. Xu, C. H. P. Wen, X. Liu, L. Shu, S. Y. Tan, X. C. Lai, Y. J. Zhang, H. Lee, V. N. Strocov, F. Bisti, P. Dudin, J.-X. Zhu, H. Q. Yuan, S. Kirchner, and D. L. Feng, Band Dependent Interlayer F-Electron Hybridization in CeRhIn<sub>5</sub>, *Phys. Rev. Lett.* **120**, 066403 (2018).
- [8] C. Petrovic, P. G. Pagliuso, M. F. Hundley, R. Movshovich, J. L. Sarrao, J. D. Thompson, Z. Fisk, and P. Monthoux, Heavy-fermion superconductivity in CeCoIn<sub>5</sub> at 2.3 K, *J. Phys.: Condens. Matter* **13**, L337 (2001).
- [9] P. Aynajian, E. H. da Silva Neto, A. Gyenis, R. E. Baumbach, J. D. Thompson, Z. Fisk, E. D. Bauer, and A. Yazdani, Visualizing heavy fermions emerging in a quantum critical Kondo lattice, *Nature (London)* **486**, 201 (2012).
- [10] M. P. Allan, F. Masee, D. K. Morr, J. Van Dyke, A. W. Rost, A. P. Mackenzie, C. Petrovic, and J. C. Davis, Imaging Cooper pairing of heavy fermions in CeCoIn<sub>5</sub>, *Nat. Phys.* **9**, 468 (2013).
- [11] B. B. Zhou, S. Misra, E. H. da Silva Neto, P. Aynajian, R. E. Baumbach, J. D. Thompson, E. D. Bauer, and A. Yazdani, Visualizing nodal heavy fermion superconductivity in CeCoIn<sub>5</sub>, *Nat. Phys.* **9**, 474 (2013).
- [12] B.-L. Young, R. R. Urbano, N. J. Curro, J. D. Thompson, J. L. Sarrao, A. B. Vorontsov, and M. J. Graf, Microscopic Evidence for Field-Induced Magnetism in CeCoIn<sub>5</sub>, *Phys. Rev. Lett.* **98**, 036402 (2007).
- [13] E. J. Singley, D. N. Basov, E. D. Bauer, and M. B. Maple, Optical conductivity of the heavy fermion superconductor CeCoIn<sub>5</sub>, *Phys. Rev. B* **65**, 161101(R) (2002).
- [14] K. Haule, C.-H. Yee, and K. Kim, Dynamical mean-field theory within the full-potential methods: Electronic structure of CeIrIn<sub>5</sub>, CeCoIn<sub>5</sub>, and CeRhIn<sub>5</sub>, *Phys. Rev. B* **81**, 195107 (2010).
- [15] Y. Tokiwa, R. Movshovich, F. Ronning, E. D. Bauer, P. Papin, A. D. Bianchi, J. F. Rauscher, S. M. Kauzlarich, and Z. Fisk, Anisotropic effect of Cd and Hg doping on the Pauli limited superconductor CeCoIn<sub>5</sub>, *Phys. Rev. B* **101**, 037001 (2008).
- [16] L. D. Pham, T. Park, S. Maquilong, J. D. Thompson, and Z. Fisk, Reversible Tuning of the Heavy-Fermion Ground State in CeCoIn<sub>5</sub>, *Phys. Rev. Lett.* **97**, 056404 (2006).
- [17] M. Nicklas, O. Stockert, T. Park, K. Habicht, K. Kiefer, L. D. Pham, J. D. Thompson, Z. Fisk, and F. Steglich, Magnetic structure of Cd-doped CeCoIn<sub>5</sub>, *Phys. Rev. B* **76**, 052401 (2007).
- [18] W. Bao, P. G. Pagliuso, J. L. Sarrao, J. D. Thompson, Z. Fisk, J. W. Lynn, and R. W. Erwin, Incommensurate magnetic structure of CeRhIn<sub>5</sub>, *Phys. Rev. B* **62**, R14621(R) (2000).
- [19] C. H. Booth, E. D. Bauer, A. D. Bianchi, F. Ronning, J. D. Thompson, J. L. Sarrao, J. Y. Cho, J. Y. Chan, C. Capan, and Z. Fisk, Local structure and site occupancy of Cd and Hg substitutions in CeTIn<sub>5</sub> (*T* = Co, Rh, and Ir), *Phys. Rev. B* **79**, 144519 (2009).

- [20] R. G. Goodrich, C. Capan, A. D. Bianchi, Z. Fisk, J. F. DiTusa, I. Vekhter, D. P. Young, L. Balicas, Y.-J. Yo, T. Murphy, J. Y. Cho, and J. Y. Chan, SC-AFM transition in  $\text{CeCo}(\text{In}_{1-x}\text{Cd}_x)_5$ : de Haas-van Alphen measurements, *J. Phys.: Conf. Ser.* **273**, 012113 (2011).
- [21] K. Gofryk, F. Ronning, J.-X. Zhu, M. N. Ou, P. H. Tobash, S. S. Stoyko, X. Lu, A. Mar, T. Park, E. D. Bauer, J. D. Thompson, and Z. Fisk, Electronic Tuning and Uniform Superconductivity in  $\text{CeCoIn}_5$ , *Phys. Rev. Lett.* **109**, 186402 (2012).
- [22] C. Capan, Y.-J. Jo, L. Balicas, R. G. Goodrich, J. F. DiTusa, I. Vekhter, T. P. Murphy, A. D. Bianchi, L. D. Pham, J. Y. Cho, J. Y. Chan, D. P. Young, and Z. Fisk, Fermi surface evolution through a heavy-fermion superconductor-to-antiferromagnet transition: de Haas-van Alphen effect in Cd-substituted  $\text{CeCoIn}_5$ , *Phys. Rev. B* **82**, 035112 (2010).
- [23] L. Howald, E. Stilp, P. Dalmas, A. Yaouanc, S. Raymond, C. Piamonteze, G. Lapertot, C. Baines, and H. Keller, Superconductivity and itinerant antiferromagnetism in the heavy fermion system  $\text{CeCo}(\text{In}_{1-x}\text{Cd}_x)_5$ , *Sci. Rep.* **5**, 12528 (2015).
- [24] H. C. Choi, B. I. Min, J. H. Shim, K. Haule, and G. Kotliar, Temperature-Dependent Fermi Surface Evolution in Heavy Fermion  $\text{CeIrIn}_5$ , *Phys. Rev. Lett.* **108**, 016402 (2012).
- [25] Q. Y. Chen, D. F. Xu, X. H. Niu, J. Jiang, R. Peng, H. C. Xu, C. H. P. Wen, Z. F. Ding, K. Huang, L. Shu, Y. J. Zhang, H. Lee, V. N. Strocov, M. Shi, F. Bisti, T. Schmitt, Y. B. Huang, P. Dudin, X. C. Lai, S. Kirchner, H. Q. Yuan, and D. L. Feng, Direct observation of how the heavy-fermion state develops in  $\text{CeCoIn}_5$ , *Phys. Rev. B* **96**, 045107 (2017).
- [26] H. Shishido, R. Settai, D. Aoki, S. Ikeda, N. Nakamura, T. Iizuka, Y. Inada, K. Sugiyama, T. Takeuchi, K. Kindo, T. C. Kobayashi, Y. Haga, H. Harima, Y. Aoki, T. Namiki, H. Sato, and Y. Onuki, Fermi surface, magnetic and superconducting properties of  $\text{LaRhIn}_5$  and  $\text{CeTIn}_5$  (T: Co, Rh, and Ir), *J. Phys. Soc. Jpn.* **71**, 162 (2002).
- [27] Q. Y. Chen, C. H. P. Wen, Q. Yao, K. Huang, Z. F. Ding, L. Shu, X. H. Niu, Y. Zhang, X. C. Lai, Y. B. Huang, G. B. Zhang, S. Kirchner, and D. L. Feng, Tracing crystal-field splittings in the rare-earth-based intermetallic  $\text{CeIrIn}_5$ , *Phys. Rev. B* **97**, 045149 (2018).
- [28] S. Patil, A. Generalov, M. Guttler, P. Kushwaha, A. Chikina, K. Kummer, T. C. Rodel, A. F. Santander-Syro, N. Caroca-Canales, C. Geibel, S. Danzenbacher, Y. Kucherenko, C. Laubschat, J. W. Allen, and D. V. Vyalikh, APRES view on surface and bulk hybridization phenomena in the antiferromagnetic Kondo lattice  $\text{CeRh}_2\text{Si}_2$ , *Nat. Commun.* **7**, 11029 (2016).
- [29] S. Jang, R. Kealhofer, C. John, S. Doyle, J.-S. Hong, J.-H. Shim, Q. Si, J. D. Denlinger, and J. G. Analytis, Direct visualization of coexisting channels of interaction in  $\text{CeSb}$ , *Sci. Adv.* **5**, eaat7158 (2019).
- [30] See Supplemental Material at <http://link.aps.org/supplemental/10.1103/PhysRevB.100.235148> for Suppression of hybridization by Cd doping in  $\text{CeCoIn}_5$ , which includes Ref. [31].
- [31] H. C. Xu, Y. Zhang, M. Xu, R. Peng, X. P. Shen, V. N. Strocov, M. Shi, M. Kobayashi, T. Schmitt, B. P. Xie, and D. L. Feng, Direct Observation of the Bandwidth Control Mott Transition in the  $\text{NiS}_{2-x}\text{Se}_x$  Multiband System, *Phys. Rev. Lett.* **112**, 087603 (2014).
- [32] J. H. Shim, K. Haule, and G. Kotliar, Modeling the localized-to-itinerant electronic transition in the heavy fermion system  $\text{CeIrIn}_5$ , *Science* **318**, 1615 (2007).
- [33] T. Willers, F. Strigari, Z. Hu, W. Sessi, N. B. Brookes, E. D. Bauer, J. L. Sarrao, J. D. Thompson, A. Tanaka, S. Wirth, L. H. Tjeng, and A. Severing, Correlation between ground state and orbital anisotropy in heavy fermion materials? *Proc. Natl. Acad. Sci. USA* **112**, 2384 (2015).
- [34] M. Haze, R. Peters, Y. Torii, T. Suematsu, D. Sano, M. Naritsuka, Y. Kasahara, T. Shibauchi, T. Terashima, and Y. Matsuda, Direct evidence for the existence of heavy quasiparticles in the magnetically ordered phase of  $\text{CeRhIn}_5$ , *J. Phys. Soc. Jpn.* **88**, 014706 (2019).
- [35] Q. Y. Chen, X. B. Luo, M. L. Li, X. Y. Ji, R. Zhou, Y. B. Huang, W. Zhang, W. Feng, Y. Zhang, L. Huang, Q. Q. Hao, Q. Liu, X. G. Zhu, Y. Liu, P. Zhang, X. C. Lai, Q. Si, and S. Y. Tan, Orbital-Selective Kondo Entanglement and Antiferromagnetic Order in  $\text{USb}_2$ , *Phys. Rev. Lett.* **123**, 106402 (2019).
- [36] H. Sakai, F. Ronning, J.-X. Zhu, N. Wakeham, H. Yasuoka, Y. Tokunaga, S. Kambe, E. D. Bauer, and J. D. Thompson, Microscopic investigation of electronic inhomogeneity induced by substitutions in a quantum critical metal  $\text{CeCoIn}_5$ , *Phys. Rev. B* **92**, 121105(R) (2015).
- [37] R. R. Urbano, B.-L. Young, N. J. Curro, J. D. Thompson, L. D. Pham, and Z. Fisk, Interacting Antiferromagnetic Droplets in Quantum Critical  $\text{CeCoIn}_5$ , *Phys. Rev. Lett.* **99**, 146402 (2007).